

Object Detection

Milan Straka

 April 06, 2020



EUROPEAN UNION
European Structural and Investment Fund
Operational Programme Research,
Development and Education

Charles University in Prague
Faculty of Mathematics and Physics
Institute of Formal and Applied Linguistics



unless otherwise stated

Beyond Image Classification

Beyond Image Classification

- Object detection (including location)

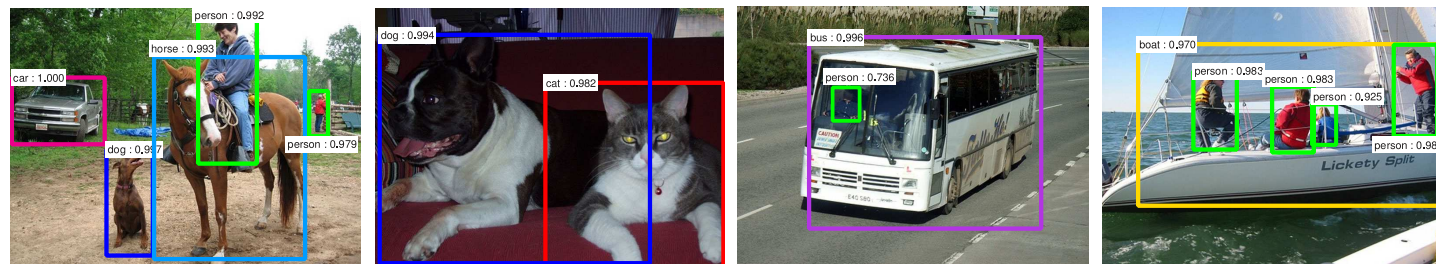


Figure 3 of paper "Faster R-CNN: Towards Real-Time Object Detection with Region Proposal Networks", <https://arxiv.org/abs/1506.01497>

- Image segmentation

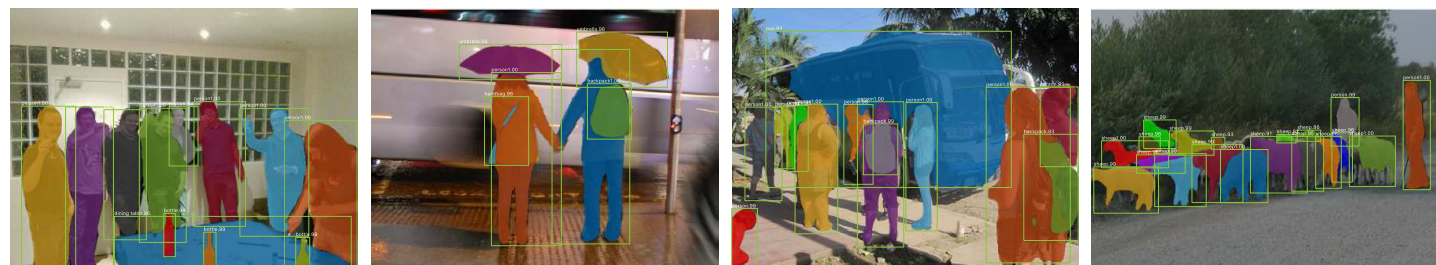


Figure 2 of paper "Mask R-CNN", <https://arxiv.org/abs/1703.06870>.

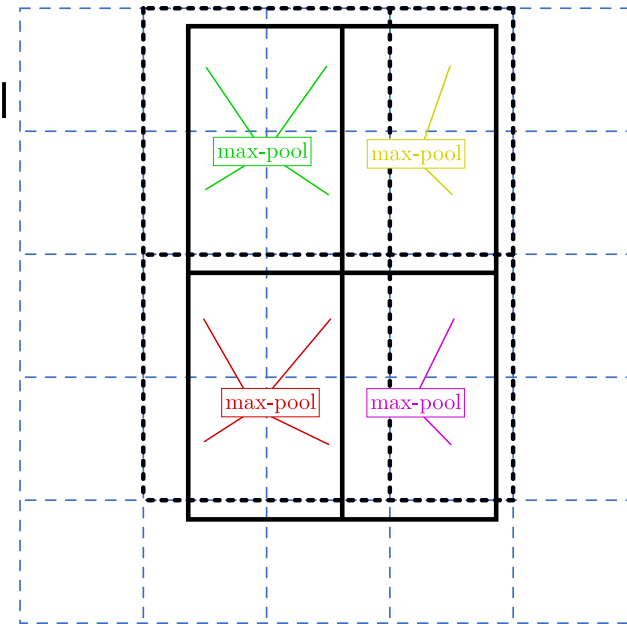
- Human pose estimation



Figure 7 of paper "Mask R-CNN", <https://arxiv.org/abs/1703.06870>.

Fast R-CNN Architecture

- Start with a network pre-trained on ImageNet (VGG-16 is used in the original paper).
- Several rectangular **Regions of Interest (RoI)** are passed on the input. For every of them, the network decides whether:
 - they contain an object;
 - location of the object relative to the RoI.
- RoI representation is *fixed size*, independent on its size. It is computed using **RoI pooling**, which replaces the last max-pool layer ($14 \times 14 \rightarrow 7 \times 7$ in VGG). For each channel, the representation of each RoI *bin* (one of the 7×7) is computed as max-pool of the corresponding bins (of the 14×14 grid in VGG) of the convolutional image features.
- For every RoI, two sibling heads are added:
 - *classification head* predicts one of $K + 1$ categories;
 - *bounding box regression head* predicts 4 bounding box parameters.



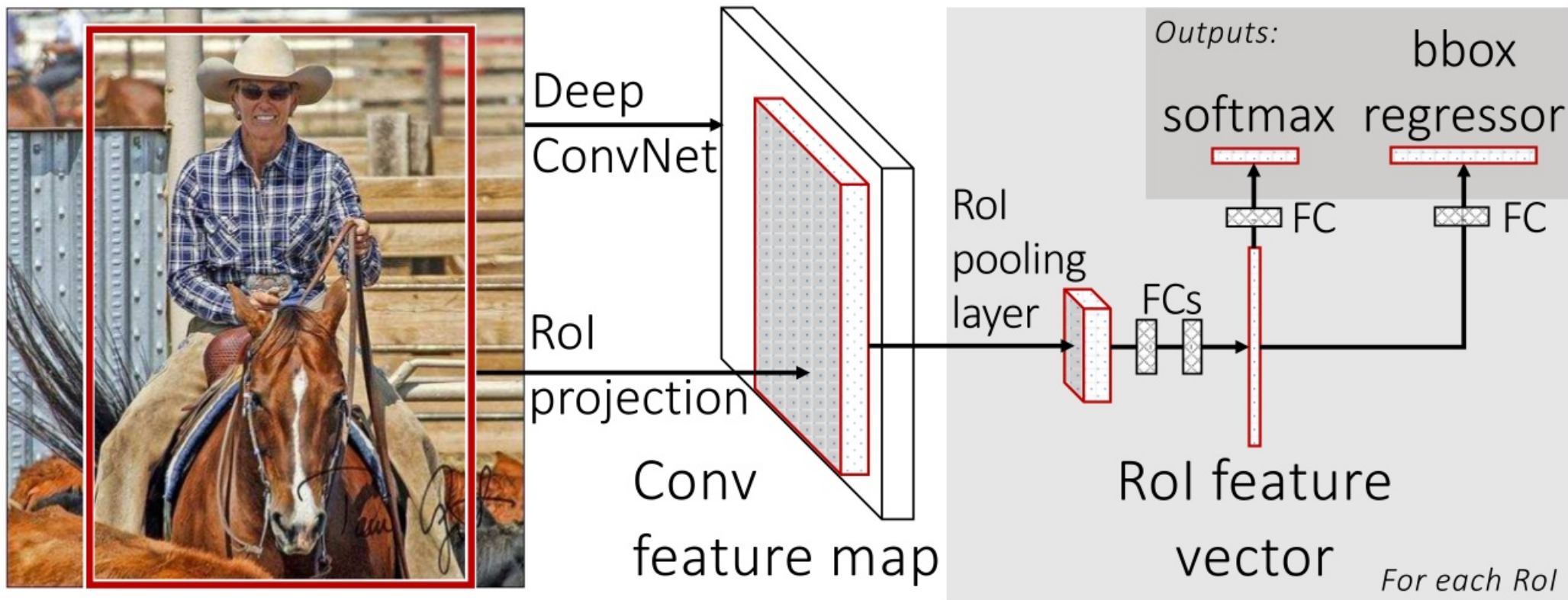


Figure 1 of paper "Fast R-CNN", <https://arxiv.org/abs/1504.08083>.

The bounding box is parametrized as follows. Let x_r, y_r, w_r, h_r be center coordinates and width and height of the RoI, and let x, y, w, h be parameters of the bounding box. We represent the bounding box relative to the RoI as follows:

$$t_x = (x - x_r)/w_r, \quad t_y = (y - y_r)/h_r$$

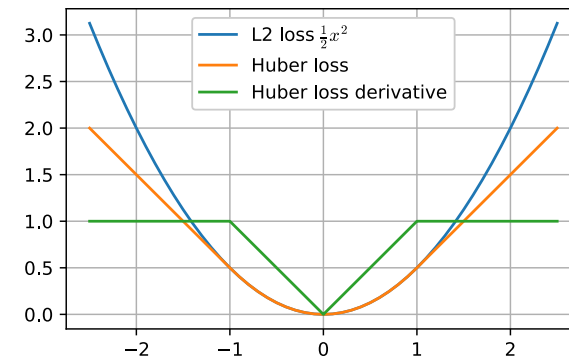
$$t_w = \log(w/w_r), \quad t_h = \log(h/h_r)$$

Usually a smooth_{L_1} loss, or *Huber loss*, is employed for bounding box parameters

$$\text{smooth}_{L_1}(x) = \begin{cases} 0.5x^2 & \text{if } |x| < 1 \\ |x| - 0.5 & \text{otherwise} \end{cases}$$

The complete loss is then

$$L(\hat{c}, \hat{t}, c, t) = L_{\text{cls}}(\hat{c}, c) + \lambda \cdot [c \geq 1] \cdot \sum_{i \in \{x, y, w, h\}} \text{smooth}_{L_1}(\hat{t}_i - t_i).$$



Intersection over union

For two bounding boxes (or two masks) the *intersection over union* (*IoU*) is a ration of the intersection of the boxes (or masks) and the union of the boxes (or masks).

Choosing Rols for training

During training, we use 2 images with 64 Rols each. The Rols are selected so that 25% have intersection over union (IoU) overlap with ground-truth boxes at least 0.5; the others are chosen to have the IoU in range $[0.1, 0.5)$, the so-called *hard examples*.

Choosing Rols during inference

Single object can be found in multiple Rols. To choose the most salient one, we perform *non-maximum suppression* – we ignore Rols which have an overlap with a higher scoring Rol of the same type, where the IoU is larger than a given threshold (usually, 0.3 is used). Higher scoring Rol is the one with higher probability from the classification head.

Average Precision

Evaluation is performed using *Average Precision* (AP or AP_{50}).

We assume all bounding boxes (or masks) produced by a system have confidence values which can be used to rank them. Then, for a single class, we take the boxes (or masks) in the order of the ranks and generate precision/recall curve, considering a bounding box correct if it has IoU at least 0.5 with any ground-truth box.

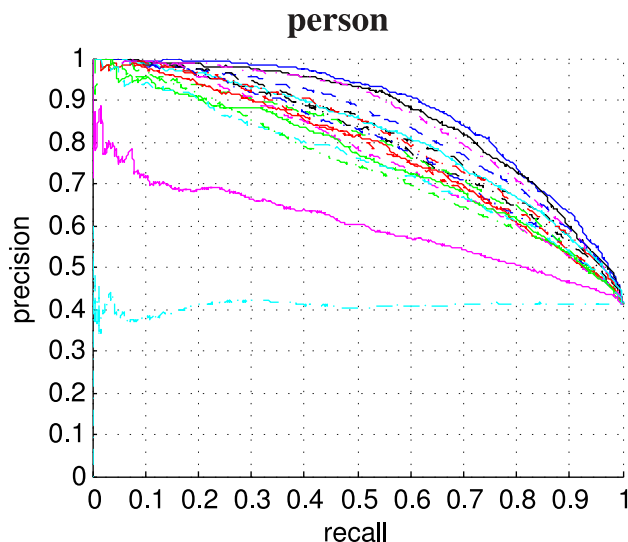


Figure 6 of paper "The PASCAL Visual Object Classes (VOC) Challenge", http://homepages.inf.ed.ac.uk/ckiwi/postscript/ijcv_voc09.pdf.

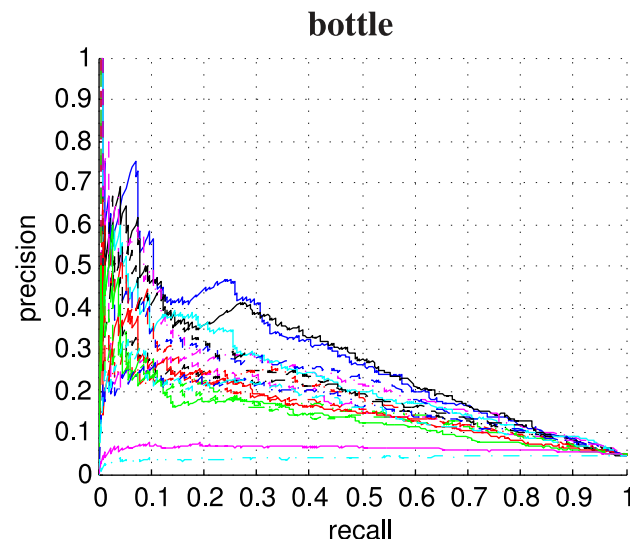
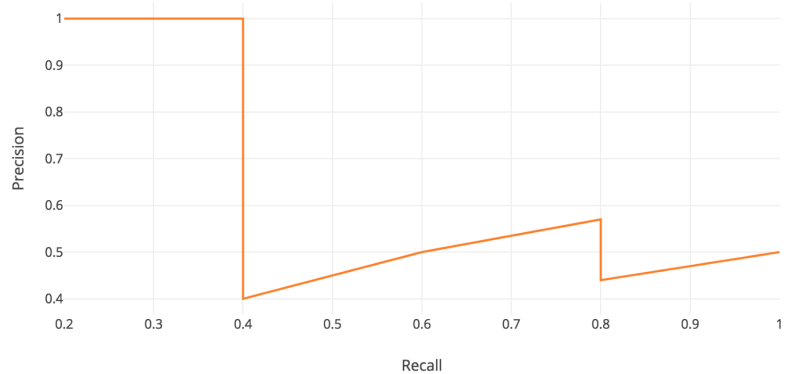


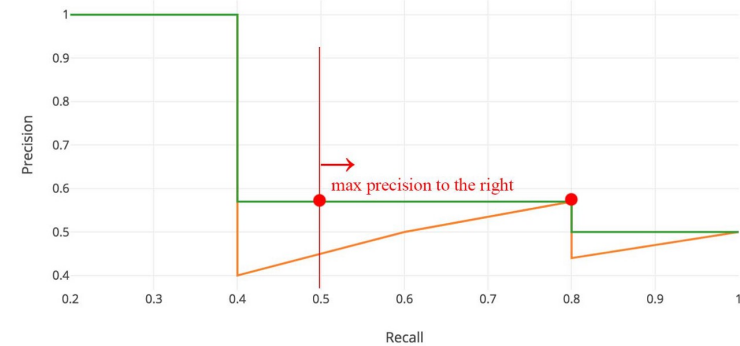
Figure 6 of paper "The PASCAL Visual Object Classes (VOC) Challenge", http://homepages.inf.ed.ac.uk/ckiwi/postscript/ijcv_voc09.pdf.

Object Detection Evaluation – Average Precision

The general ideal of AP is to compute the area under the precision/recall curve.



https://miro.medium.com/max/1400/1*VenTq4lgxjmlpOXWdFb-jg.png

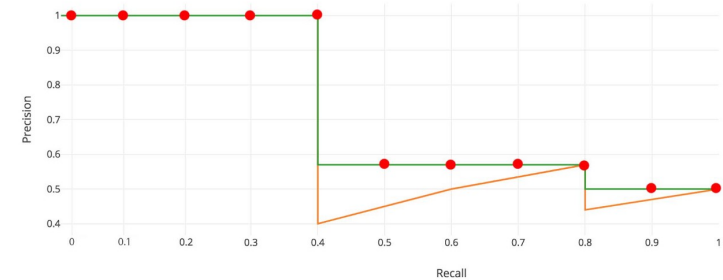


https://miro.medium.com/max/1400/1*pmSxeb4EfdGnzT6Xa68GEQ.jpeg

We start by interpolating the precision/recall curve, so that it is always non-increasing.

Finally, the average precision for a single class is an average of precision at recall 0.0, 0.1, 0.2, ..., 1.0.

The final AP is a mean of average precision of all classes.



https://miro.medium.com/max/1400/1*naz02wO-XMywlwAdFzF-GA.jpeg

Object Detection Evaluation – Average Precision

For the COCO dataset, the AP is computed slightly differently. First, it is an average over 101 recall points $0.00, 0.01, 0.02, \dots, 1.00$.

In the original metric, IoU of 50% is enough to consider the prediction valid. We can generalize the definition to AP_x , where an object prediction is considered valid if IoU is at least x .

The main COCO metric, denoted just AP , is the mean of $AP_{50}, AP_{55}, AP_{60}, \dots, AP_{95}$.

Metric	Description
AP	Mean of $AP_{50}, AP_{55}, AP_{60}, AP_{65}, \dots, AP_{95}$
AP_{50}	AP at IoU 50%
AP_{75}	AP at IoU 75%
AP_S	AP for small objects: $area < 32^2$
AP_M	AP for medium objects: $32^2 < area < 96^2$
AP_L	AP for large objects: $96^2 < area$

For Fast R-CNN, the most time consuming part is generating the Rols.

Therefore, Faster R-CNN jointly generates *regions of interest* using a *region proposal network* and performs object detection.

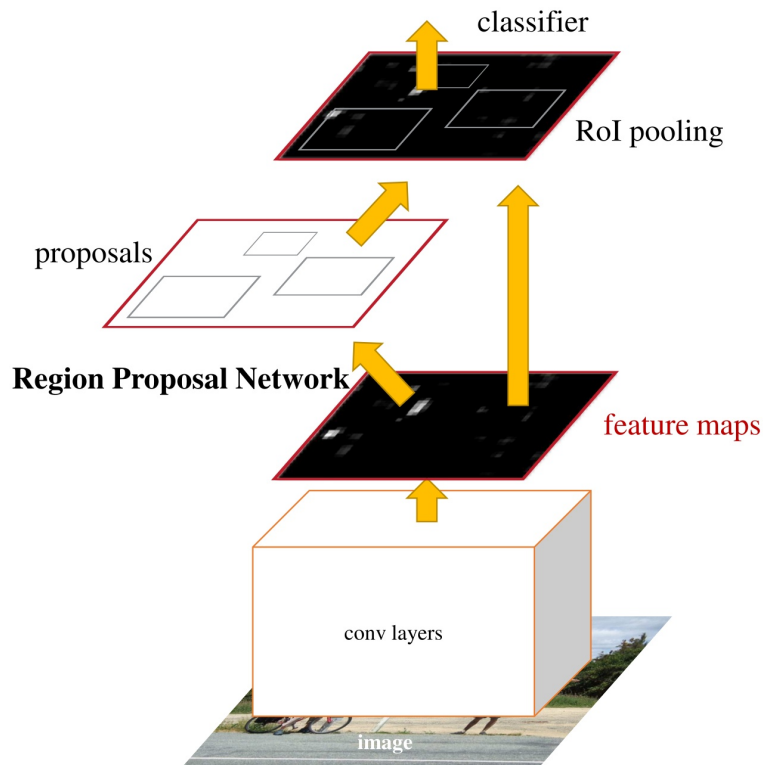


Figure 2 of paper "Faster R-CNN: Towards Real-Time Object Detection with Region Proposal Networks", <https://arxiv.org/abs/1506.01497>

The region proposals are generated using a 3×3 sliding window, with 3 different scales ($128^2, 256^2, 512^2$) and 3 aspect ratios ($1 : 1, 1 : 2, 2 : 1$). For every anchor, there is a FastR-CNN-like object detection head – a classification into two classes (background, object) and a boundary regressor.

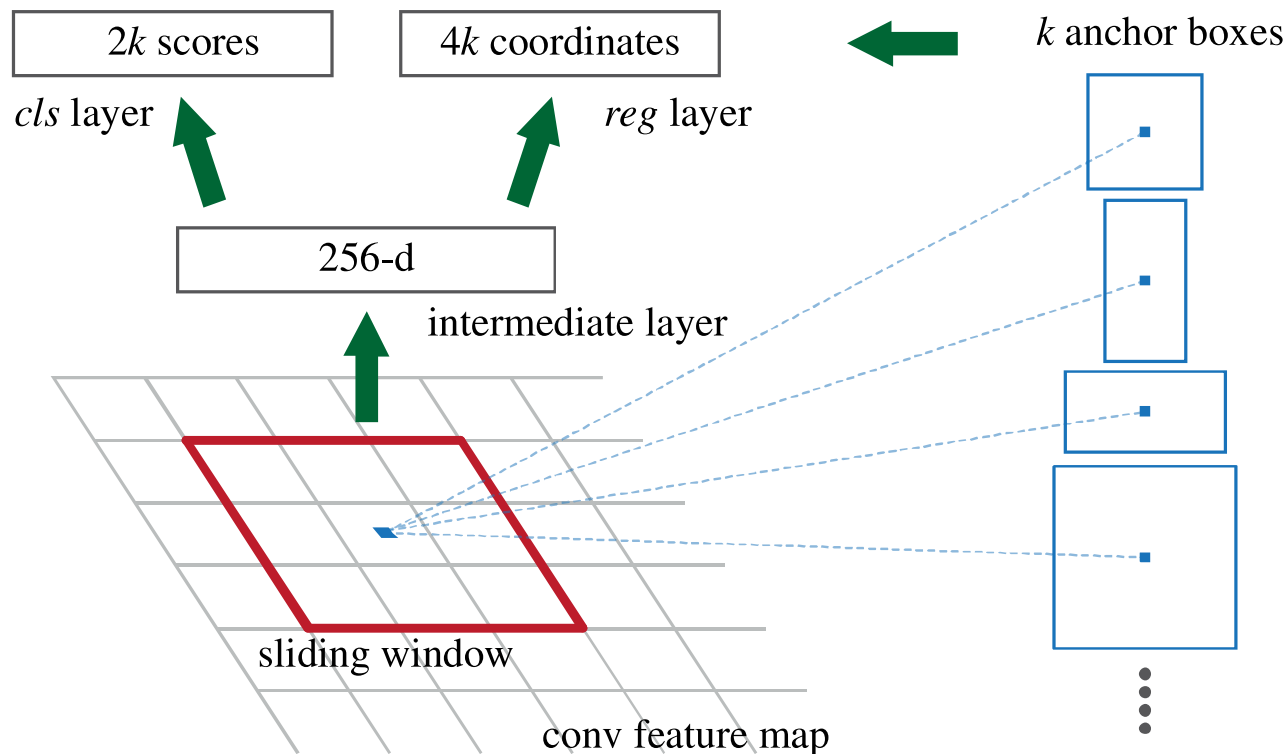


Figure 3 of paper "Faster R-CNN: Towards Real-Time Object Detection with Region Proposal Networks", <https://arxiv.org/abs/1506.01497>

During training, we generate

- positive training examples for every anchor that has highest IoU with a ground-truth box;
- furthermore, a positive example is also any anchor with IoU at least 0.7 for any ground-truth box;
- negative training examples for every anchor that has IoU at most 0.3 with all ground-truth boxes.

During inference, we consider all predicted non-background regions, run non-maximum suppression on them using a 0.7 IoU threshold, and then take N top-scored regions (i.e., the ones with highest probability from the classification head) – the paper uses 300 proposals, compared to 2000 in the Fast R-CNN.

Table 3: Detection results on **PASCAL VOC 2007 test set**. The detector is Fast R-CNN and VGG-16. Training data: “07”: VOC 2007 trainval, “07+12”: union set of VOC 2007 trainval and VOC 2012 trainval. For RPN, the train-time proposals for Fast R-CNN are 2000. †: this number was reported in [2]; using the repository provided by this paper, this result is higher (68.1).

method	# proposals	data	mAP (%)
SS	2000	07	66.9 [†]
SS	2000	07+12	70.0
RPN+VGG, unshared	300	07	68.5
RPN+VGG, shared	300	07	69.9
RPN+VGG, shared	300	07+12	73.2
RPN+VGG, shared	300	COCO+07+12	78.8

Table 4: Detection results on **PASCAL VOC 2012 test set**. The detector is Fast R-CNN and VGG-16. Training data: “07”: VOC 2007 trainval, “07++12”: union set of VOC 2007 trainval+test and VOC 2012 trainval. For RPN, the train-time proposals for Fast R-CNN are 2000. †: <http://host.robots.ox.ac.uk:8080/anonymous/HZJTQA.html>. ‡: <http://host.robots.ox.ac.uk:8080/anonymous/YNPLXB.html>. §: <http://host.robots.ox.ac.uk:8080/anonymous/XEDH10.html>.

method	# proposals	data	mAP (%)
SS	2000	12	65.7
SS	2000	07++12	68.4
RPN+VGG, shared [†]	300	12	67.0
RPN+VGG, shared [‡]	300	07++12	70.4
RPN+VGG, shared [§]	300	COCO+07++12	75.9

Tables 3 and 4 of paper "Faster R-CNN: Towards Real-Time Object Detection with Region Proposal Networks", <https://arxiv.org/abs/1506.01497>

The Faster R-CNN is a so-called **two-stage** detector, where the regions are refined twice – once in the region proposal network, and then in the final bounding box regressor.

Several **single-stage** detector architectures have been proposed, mainly because they are faster and smaller, but until circa 2017 the two-stage detectors achieved better results.

Mask R-CNN

Straightforward extension of Faster R-CNN able to produce image segmentation (i.e., masks for every object).

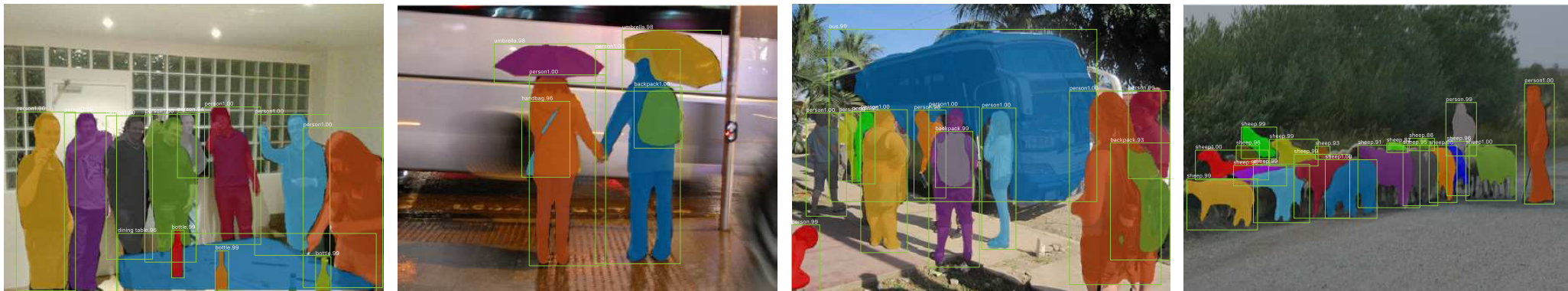


Figure 2 of paper "Mask R-CNN", <https://arxiv.org/abs/1703.06870>.

Mask R-CNN – Architecture

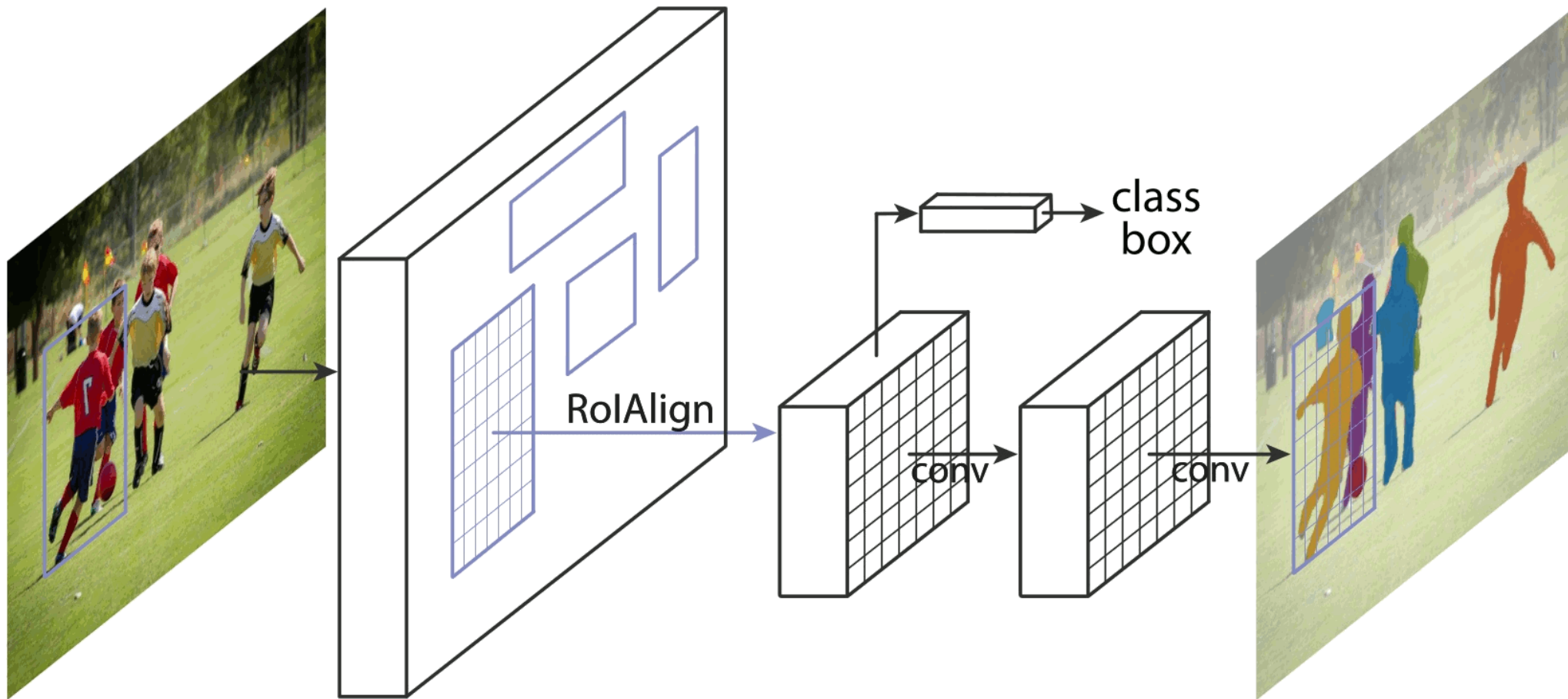


Figure 1 of paper "Mask R-CNN", <https://arxiv.org/abs/1703.06870>.

Mask R-CNN – RoIAlign

More precise alignment is required for the RoI in order to predict the masks. Instead of quantization and max-pooling in RoI pooling, **RoIAlign** uses bilinear interpolation of features at four regularly samples locations in each RoI bin and averages them.

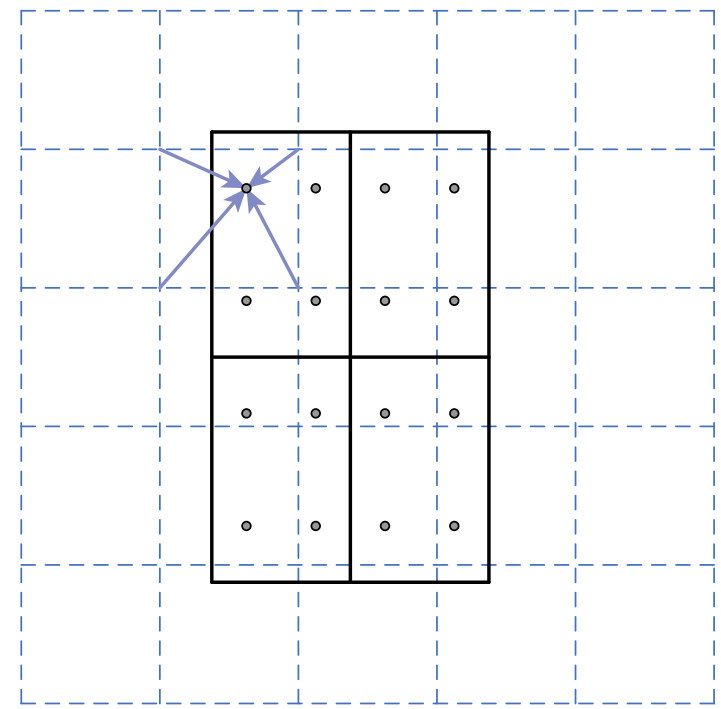
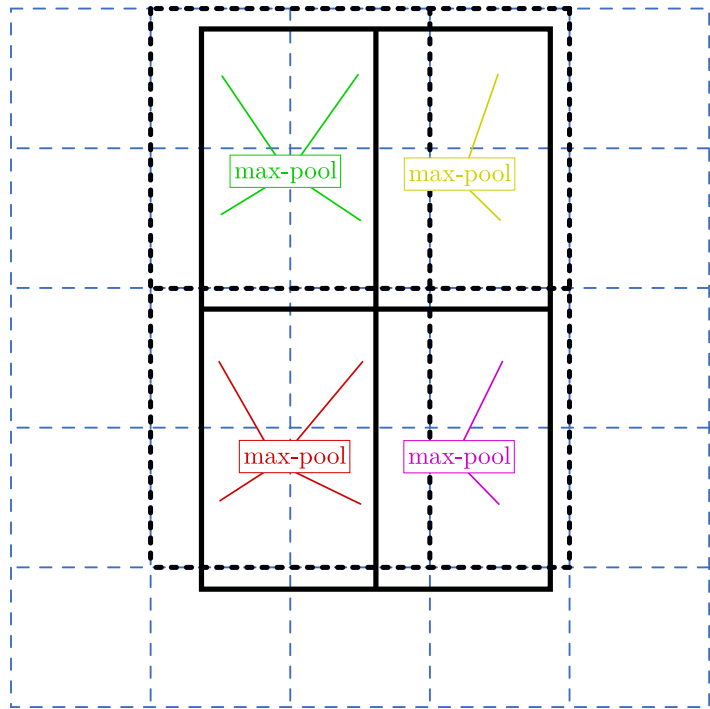


Figure 3 of paper "Mask R-CNN", <https://arxiv.org/abs/1703.06870>.

TensorFlow provides `tf.image.crop_and_resize` capable of implementing RoIAlign.

Mask R-CNN

Masks are predicted in a third branch of the object detector.

- Usually higher resolution is needed (14×14 instead of 7×7).
- The masks are predicted for each class separately.
- The masks are predicted using convolutions instead of fully connected layers.

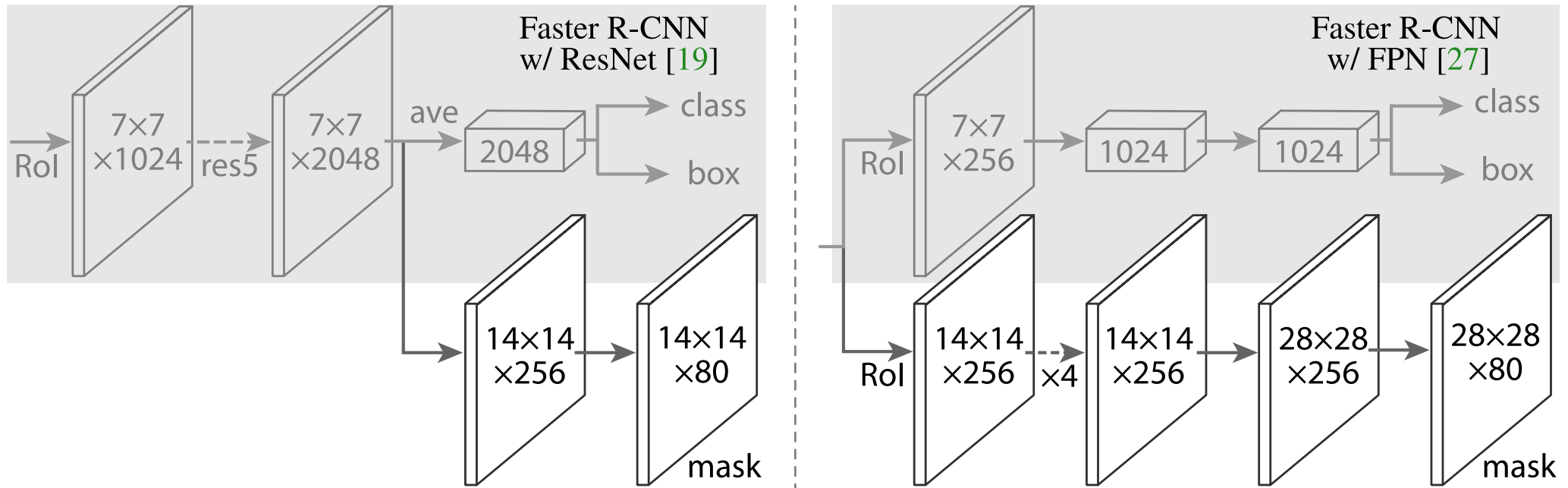


Figure 4 of paper "Mask R-CNN", <https://arxiv.org/abs/1703.06870>.

<i>net-depth-features</i>	AP	AP ₅₀	AP ₇₅
ResNet-50-C4	30.3	51.2	31.5
ResNet-101-C4	32.7	54.2	34.3
ResNet-50-FPN	33.6	55.2	35.3
ResNet-101-FPN	35.4	57.3	37.5
ResNeXt-101-FPN	36.7	59.5	38.9

(a) **Backbone Architecture:** Better backbones bring expected gains: deeper networks do better, FPN outperforms C4 features, and ResNeXt improves on ResNet.

	AP	AP ₅₀	AP ₇₅
<i>softmax</i>	24.8	44.1	25.1
<i>sigmoid</i>	30.3	51.2	31.5
	+5.5	+7.1	+6.4

(b) **Multinomial vs. Independent Masks (ResNet-50-C4):** *Decoupling* via per-class binary masks (sigmoid) gives large gains over multinomial masks (softmax).

	align?	bilinear?	agg.	AP	AP ₅₀	AP ₇₅
<i>RoIPool</i> [12]			max	26.9	48.8	26.4
<i>RoIWarp</i> [10]		✓	max	27.2	49.2	27.1
		✓	ave	27.1	48.9	27.1
<i>RoIAlign</i>	✓	✓	max	30.2	51.0	31.8
	✓	✓	ave	30.3	51.2	31.5

(c) **RoIAlign (ResNet-50-C4):** Mask results with various RoI layers. Our RoIAlign layer improves AP by ~ 3 points and AP₇₅ by ~ 5 points. Using proper alignment is the only factor that contributes to the large gap between RoI layers.

	AP	AP ₅₀	AP ₇₅	AP ^{bb}	AP ₅₀ ^{bb}	AP ₇₅ ^{bb}
<i>RoIPool</i>	23.6	46.5	21.6	28.2	52.7	26.9
<i>RoIAlign</i>	30.9	51.8	32.1	34.0	55.3	36.4
	+7.3	+5.3	+10.5	+5.8	+2.6	+9.5

(d) **RoIAlign (ResNet-50-C5, stride 32):** Mask-level and box-level AP using *large-stride* features. Misalignments are more severe than with stride-16 features (Table 2c), resulting in big accuracy gaps.

	mask branch	AP	AP ₅₀	AP ₇₅
MLP	fc: 1024 \rightarrow 1024 \rightarrow 80 \cdot 28 ²	31.5	53.7	32.8
MLP	fc: 1024 \rightarrow 1024 \rightarrow 1024 \rightarrow 80 \cdot 28 ²	31.5	54.0	32.6
FCN	conv: 256 \rightarrow 256 \rightarrow 256 \rightarrow 256 \rightarrow 256 \rightarrow 80	33.6	55.2	35.3

(e) **Mask Branch (ResNet-50-FPN):** Fully convolutional networks (FCN) vs. multi-layer perceptrons (MLP, fully-connected) for mask prediction. FCNs improve results as they take advantage of explicitly encoding spatial layout.

Table 2. **Ablations.** We train on `trainval35k`, test on `minival`, and report *mask* AP unless otherwise noted.

Table 2 of paper "Mask R-CNN", <https://arxiv.org/abs/1703.06870>.

Mask R-CNN – Human Pose Estimation



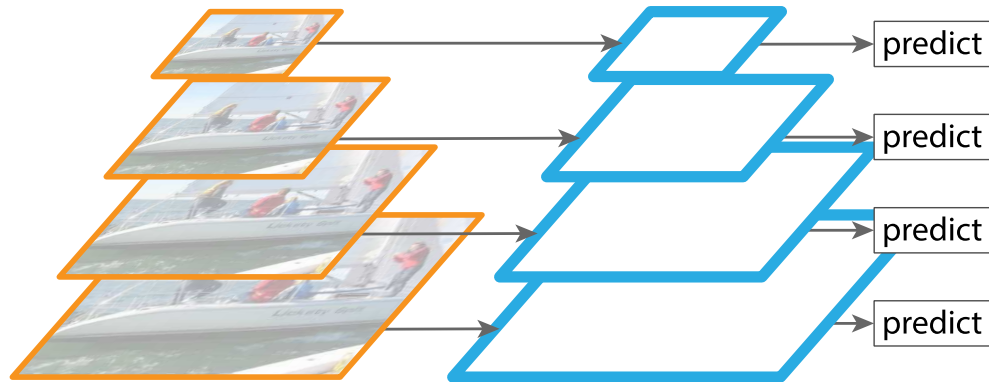
Figure 7 of paper "Mask R-CNN", <https://arxiv.org/abs/1703.06870>.

- Testing applicability of Mask R-CNN architecture.
- Keypoints (e.g., left shoulder, right elbow, ...) are detected as independent one-hot masks of size 56×56 with softmax output function.

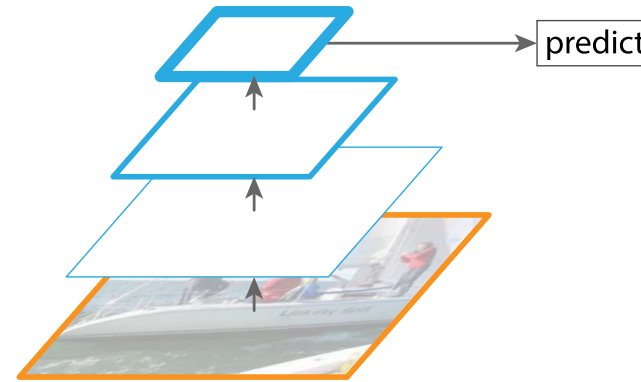
	AP^{kp}	AP_{50}^{kp}	AP_{75}^{kp}	AP_M^{kp}	AP_L^{kp}
CMU-Pose+++ [6]	61.8	84.9	67.5	57.1	68.2
G-RMI [32] [†]	62.4	84.0	68.5	59.1	68.1
Mask R-CNN, keypoint-only	62.7	87.0	68.4	57.4	71.1
Mask R-CNN, keypoint & mask	63.1	87.3	68.7	57.8	71.4

Table 4 of paper "Mask R-CNN", <https://arxiv.org/abs/1703.06870>.

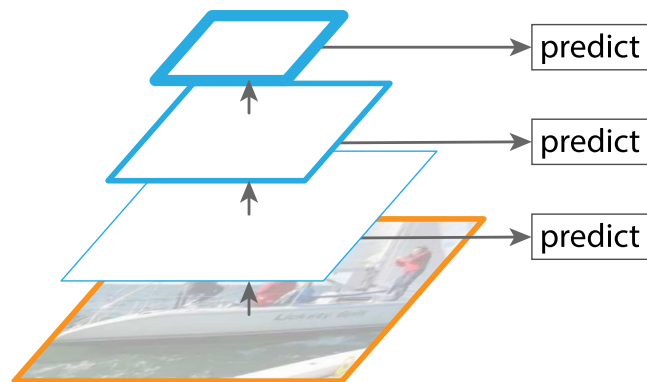
Feature Pyramid Networks



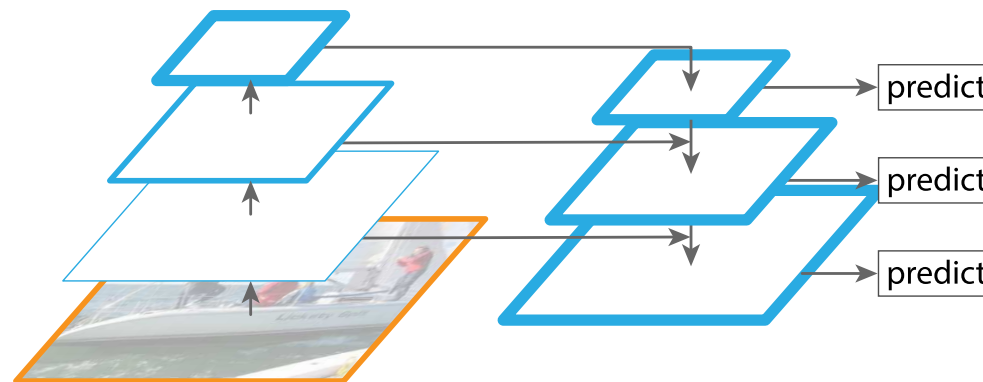
(a) Featurized image pyramid



(b) Single feature map



(c) Pyramidal feature hierarchy



(d) Feature Pyramid Network

Figure 1 of paper "Feature Pyramid Networks for Object Detection", <https://arxiv.org/abs/1612.03144>.

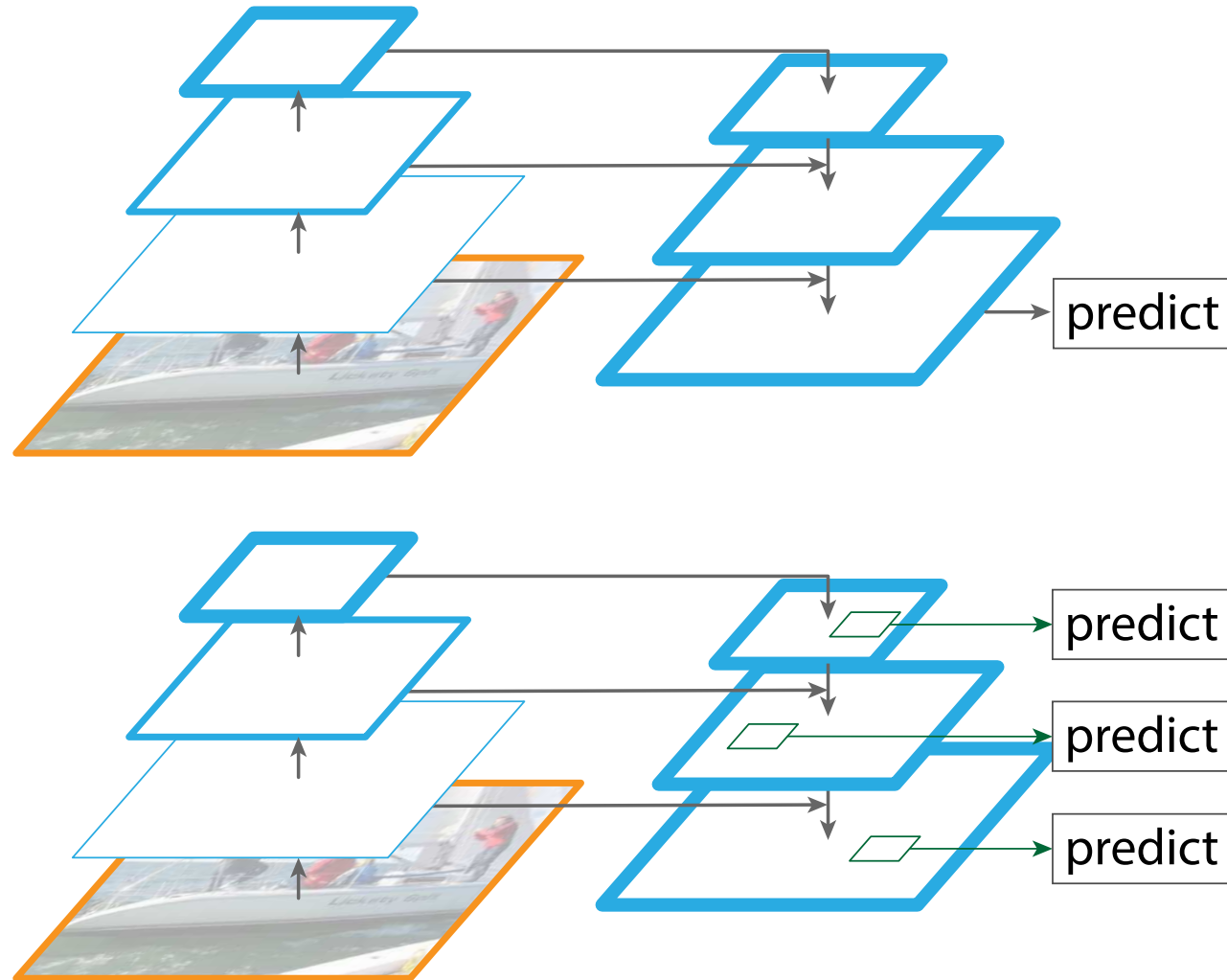


Figure 2 of paper "Feature Pyramid Networks for Object Detection", <https://arxiv.org/abs/1612.03144>.

Feature Pyramid Networks

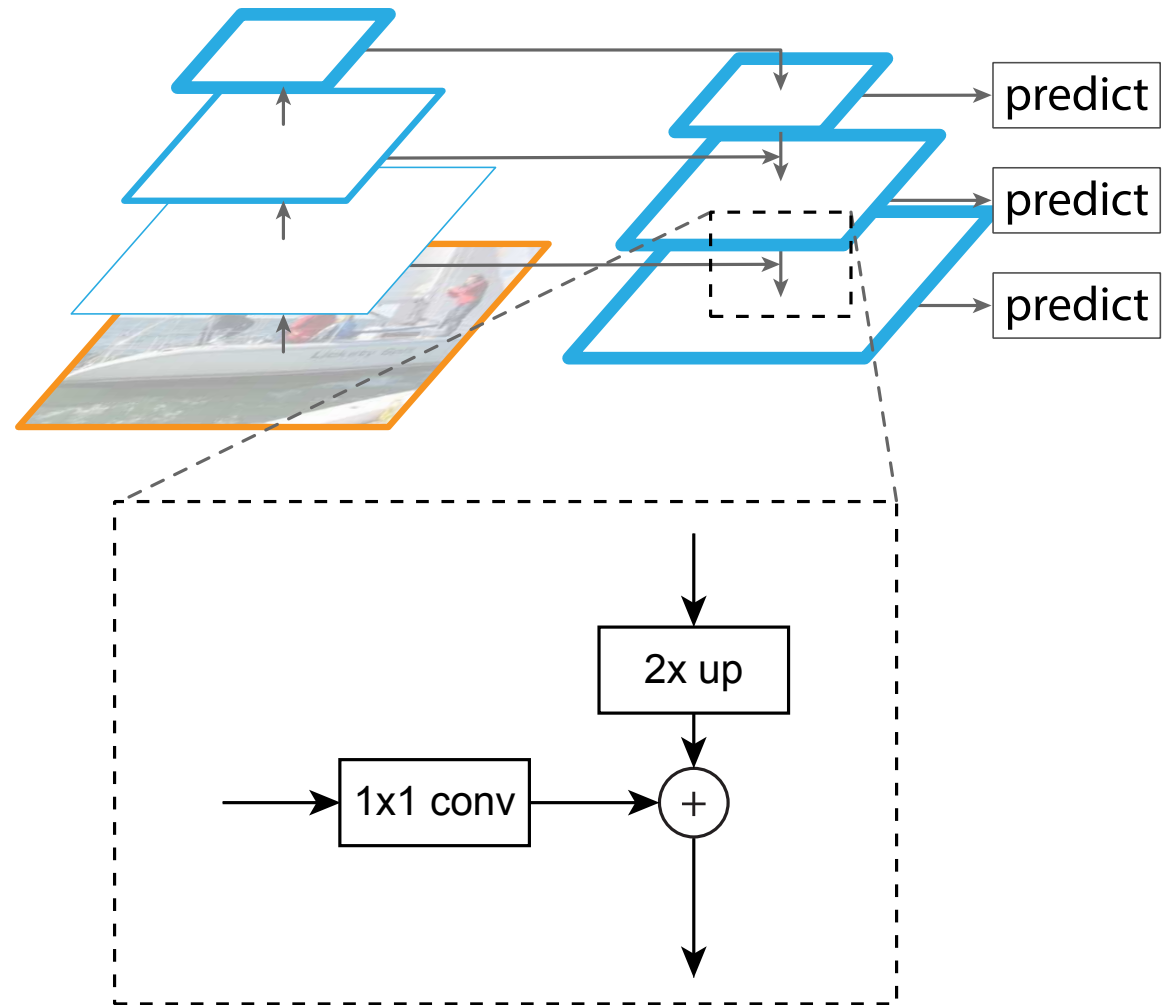


Figure 3 of paper "Feature Pyramid Networks for Object Detection", <https://arxiv.org/abs/1612.03144>.

Feature Pyramid Networks

We employ FPN as a backbone in Faster R-CNN.

Assuming ResNet-like network with 224×224 input, we denote C_2, C_3, \dots, C_5 the image features of the last convolutional layer of size $56 \times 56, 28 \times 28, \dots, 7 \times 7$ (i.e., C_i indicates a downscaling of 2^i). The FPN representations incorporating the smaller resolution features are denoted as P_2, \dots, P_5 , each consisting of 256 channels.

In both the RPN and the Fast R-CNN, authors utilize the P_2, \dots, P_5 representations, considering single-size anchors for every P_i (of size $32^2, 64^2, 128^2, 256^2$, respectively). However, three aspect ratios ($1 : 1, 1 : 2, 2 : 1$) are still used.

method	backbone	competition	image pyramid	test-dev					test-std				
				AP@.5	AP	AP _s	AP _m	AP _l	AP@.5	AP	AP _s	AP _m	AP _l
ours, Faster R-CNN on FPN	ResNet-101	-		59.1	36.2	18.2	39.0	48.2	58.5	35.8	17.5	38.7	47.8

Competition-winning single-model results follow:

G-RMI [†]	Inception-ResNet	2016		-	34.7	-	-	-	-	-	-	-	-
AttractionNet [‡] [10]	VGG16 + Wide ResNet [§]	2016	✓	53.4	35.7	15.6	38.0	52.7	52.9	35.3	14.7	37.6	51.9
Faster R-CNN +++ [16]	ResNet-101	2015	✓	55.7	34.9	15.6	38.7	50.9	-	-	-	-	-
Multipath [40] (on minival)	VGG-16	2015		49.6	31.5	-	-	-	-	-	-	-	-
ION [‡] [2]	VGG-16	2015		53.4	31.2	12.8	32.9	45.2	52.9	30.7	11.8	32.8	44.8

Table 4 of paper "Feature Pyramid Networks for Object Detection", <https://arxiv.org/abs/1612.03144>.

Focal Loss

For single-stage object detection architectures, *class imbalance* has been identified as the main issue preventing to obtain performance comparable to two-stage detectors. In a single-stage detector, there can be tens of thousands of anchors, with only dozens of useful training examples.

Cross-entropy loss is computed as

$$\mathcal{L}_{\text{cross-entropy}} = -\log p_{\text{model}}(y|x).$$

Focal-loss (loss focused on hard examples) is proposed as

$$\mathcal{L}_{\text{focal-loss}} = -(1 - p_{\text{model}}(y|x))^\gamma \cdot \log p_{\text{model}}(y|x).$$

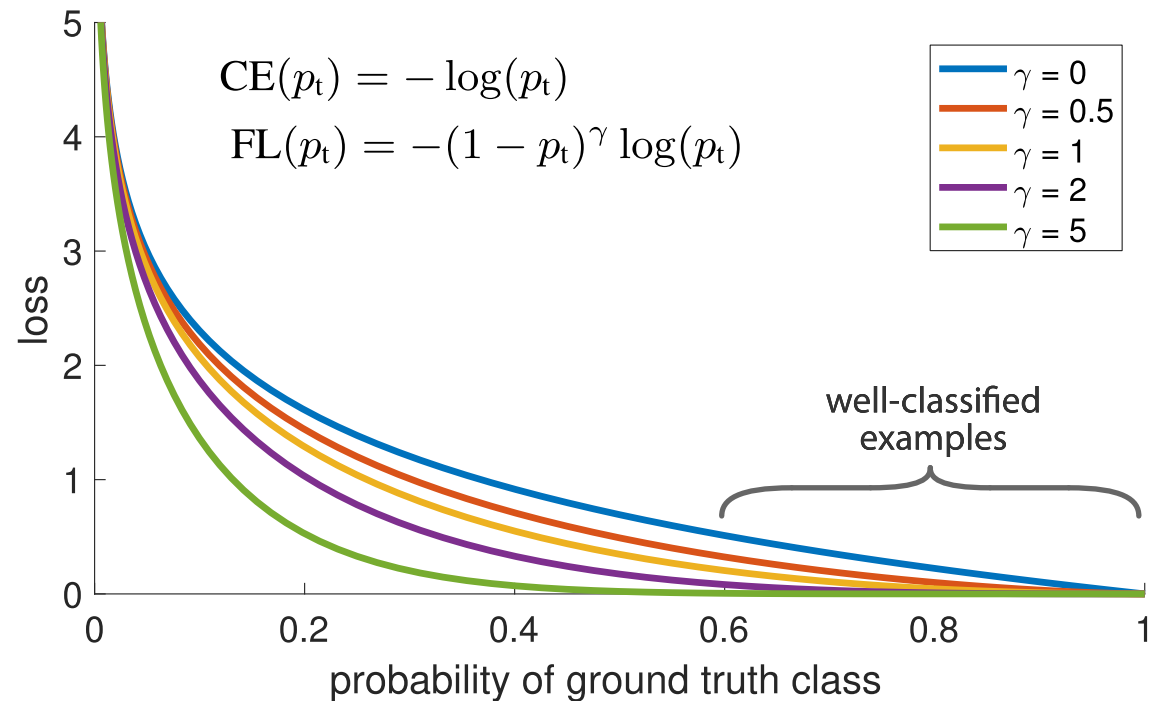


Figure 1 of paper "Focal Loss for Dense Object Detection", <https://arxiv.org/abs/1708.02002>.

For $\gamma = 0$, focal loss is equal to cross-entropy loss.

Authors reported that $\gamma = 2$ worked best for them for training a single-stage detector.

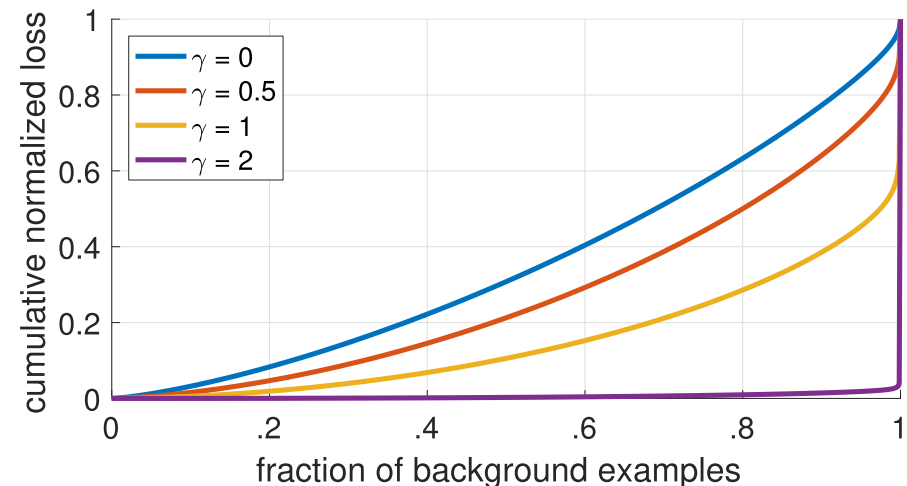
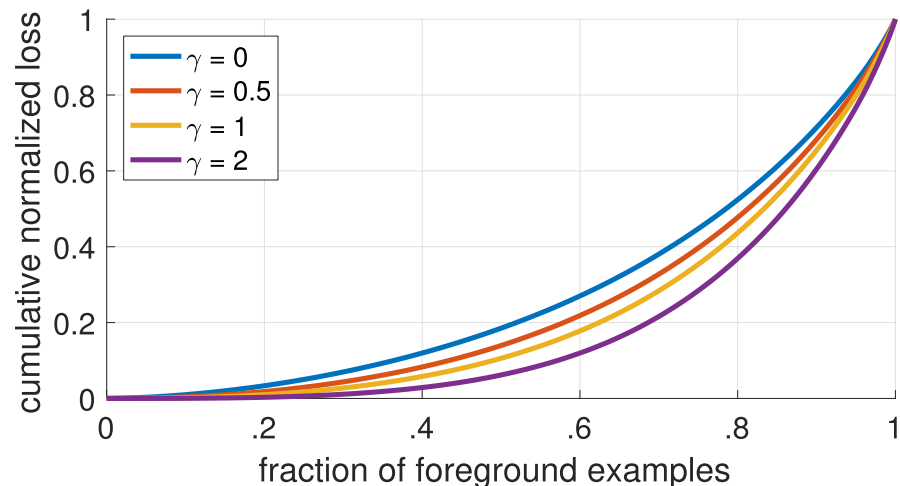


Figure 4. Cumulative distribution functions of the normalized loss for positive and negative samples for different values of γ for a *converged* model. The effect of changing γ on the distribution of the loss for positive examples is minor. For negatives, however, increasing γ heavily concentrates the loss on hard examples, focusing nearly all attention away from easy negatives.

Figure 4 of paper "Focal Loss for Dense Object Detection", <https://arxiv.org/abs/1708.02002>.

Focal Loss and Class Imbalance

Focal loss is connected to another solution to class imbalance – we might introduce weighting factor $\alpha \in (0, 1)$ for one class and $1 - \alpha$ for the other class, arriving at

$$-\alpha_y \cdot \log p_{\text{model}}(y|x).$$

The weight α might be set to the inverse class frequency or treated as a hyperparameter.

Even if weighting focus more on low-frequent class, it does not distinguish between easy and hard examples, contrary to focal loss.

In practice, the focal loss is usually used together with class weighting:

$$-\alpha_y \cdot (1 - p_{\text{model}}(y|x))^\gamma \cdot \log p_{\text{model}}(y|x).$$

For example, authors report that $\alpha = 0.25$ works best with $\gamma = 2$.

RetinaNet is a single-stage detector, using feature pyramid network architecture. Built on top of ResNet architecture, the feature pyramid contains levels P_3 through P_7 , with each P_l having 256 channels and resolution 2^l lower than the input. On each pyramid level P_l , we consider 9 anchors for every position, with 3 different aspect ratios (1, 1 : 2, 2 : 1) and with 3 different sizes ($\{2, 2^{1/3}, 2^{2/3}\} \cdot 4 \cdot 2^l$).

Note that ResNet provides only C_3 to C_5 features. C_6 is computed using a 3×3 convolution with stride 2 on C_5 , and C_7 is obtained by applying ReLU followed by another 3×3 stride-2 convolution. The C_6 and C_7 are included to improve large object detection.

RetinaNet – Architecture

The classification and boundary regression heads do not share parameters and are fully convolutional, generating *anchors · classes* sigmoids and *anchors* bounding boxes per position.

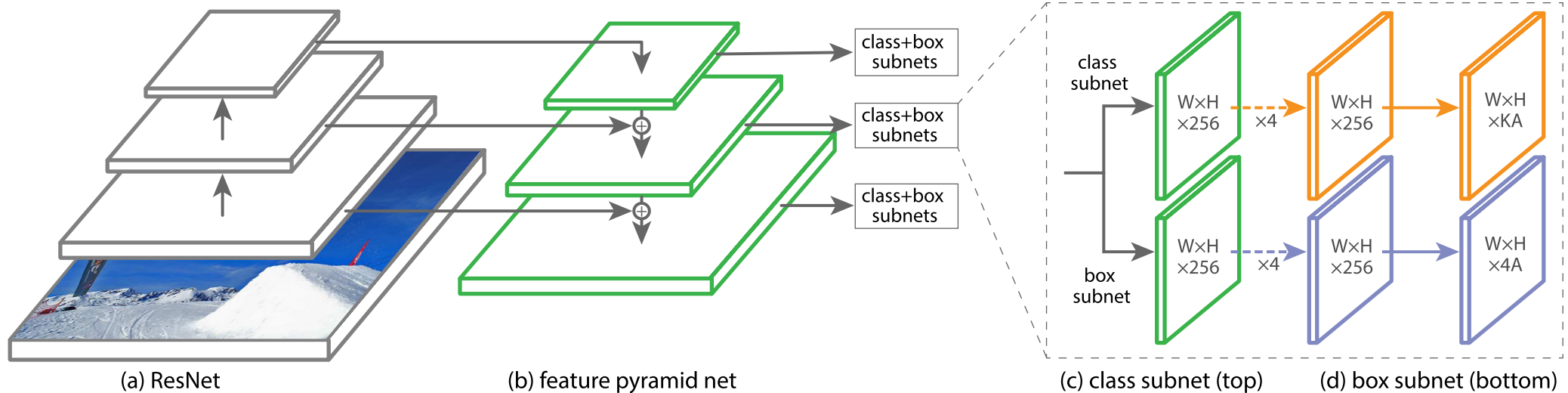


Figure 3 of paper "Focal Loss for Dense Object Detection", <https://arxiv.org/abs/1708.02002>.

During training, anchors are assigned to ground-truth object boxes if IoU is at least 0.5; to background if IoU with any ground-truth region is at most 0.4 (the rest of anchors is ignored during training). The classification head is trained using focal loss with $\gamma = 2$ and $\alpha = 0.25$ (but according to the paper, all values of γ in $[0.5, 5]$ range works well); the boundary regression head is trained using smooth_{L_1} loss as in Fast(er) R-CNN.

During inference, at most 1000 objects with at least 0.05 probability from every pyramid level are considered, and combined from all levels using non-maximum suppression with a threshold of 0.5.

	backbone	AP	AP ₅₀	AP ₇₅	AP _S	AP _M	AP _L
<i>Two-stage methods</i>							
Faster R-CNN+++ [16]	ResNet-101-C4	34.9	55.7	37.4	15.6	38.7	50.9
Faster R-CNN w FPN [20]	ResNet-101-FPN	36.2	59.1	39.0	18.2	39.0	48.2
Faster R-CNN by G-RMI [17]	Inception-ResNet-v2 [34]	34.7	55.5	36.7	13.5	38.1	52.0
Faster R-CNN w TDM [32]	Inception-ResNet-v2-TDM	36.8	57.7	39.2	16.2	39.8	52.1
<i>One-stage methods</i>							
YOLOv2 [27]	DarkNet-19 [27]	21.6	44.0	19.2	5.0	22.4	35.5
SSD513 [22, 9]	ResNet-101-SSD	31.2	50.4	33.3	10.2	34.5	49.8
DSSD513 [9]	ResNet-101-DSSD	33.2	53.3	35.2	13.0	35.4	51.1
RetinaNet (ours)	ResNet-101-FPN	39.1	59.1	42.3	21.8	42.7	50.2
RetinaNet (ours)	ResNeXt-101-FPN	40.8	61.1	44.1	24.1	44.2	51.2

Table 2 of paper "Focal Loss for Dense Object Detection", <https://arxiv.org/abs/1708.02002>.

α	AP	AP ₅₀	AP ₇₅
.10	0.0	0.0	0.0
.25	10.8	16.0	11.7
.50	30.2	46.7	32.8
.75	31.1	49.4	33.0
.90	30.8	49.7	32.3
.99	28.7	47.4	29.9
.999	25.1	41.7	26.1

(a) Varying α for CE loss ($\gamma = 0$)

γ	α	AP	AP ₅₀	AP ₇₅
0	.75	31.1	49.4	33.0
0.1	.75	31.4	49.9	33.1
0.2	.75	31.9	50.7	33.4
0.5	.50	32.9	51.7	35.2
1.0	.25	33.7	52.0	36.2
2.0	.25	34.0	52.5	36.5
5.0	.25	32.2	49.6	34.8

(b) Varying γ for FL (w. optimal α)

#sc	#ar	AP	AP ₅₀	AP ₇₅
1	1	30.3	49.0	31.8
2	1	31.9	50.0	34.0
3	1	31.8	49.4	33.7
1	3	32.4	52.3	33.9
2	3	34.2	53.1	36.5
3	3	34.0	52.5	36.5
4	3	33.8	52.1	36.2

(c) Varying anchor scales and aspects

method	batch size	nms thr	AP	AP ₅₀	AP ₇₅
OHEM	128	.7	31.1	47.2	33.2
OHEM	256	.7	31.8	48.8	33.9
OHEM	512	.7	30.6	47.0	32.6
OHEM	128	.5	32.8	50.3	35.1
OHEM	256	.5	31.0	47.4	33.0
OHEM	512	.5	27.6	42.0	29.2
OHEM 1:3	128	.5	31.1	47.2	33.2
OHEM 1:3	256	.5	28.3	42.4	30.3
OHEM 1:3	512	.5	24.0	35.5	25.8
FL	n/a	n/a	36.0	54.9	38.7

(d) FL vs. OHEM baselines (with ResNet-101-FPN)

depth	scale	AP	AP ₅₀	AP ₇₅	AP _S	AP _M	AP _L	time
50	400	30.5	47.8	32.7	11.2	33.8	46.1	64
50	500	32.5	50.9	34.8	13.9	35.8	46.7	72
50	600	34.3	53.2	36.9	16.2	37.4	47.4	98
50	700	35.1	54.2	37.7	18.0	39.3	46.4	121
50	800	35.7	55.0	38.5	18.9	38.9	46.3	153
101	400	31.9	49.5	34.1	11.6	35.8	48.5	81
101	500	34.4	53.1	36.8	14.7	38.5	49.1	90
101	600	36.0	55.2	38.7	17.4	39.6	49.7	122
101	700	37.1	56.6	39.8	19.1	40.6	49.4	154
101	800	37.8	57.5	40.8	20.2	41.1	49.2	198

(e) Accuracy/speed trade-off RetinaNet (on test-dev)

Table 1 of paper "Focal Loss for Dense Object Detection", <https://arxiv.org/abs/1708.02002>.

EfficientDet – Architecture

EfficientDet builds up on EfficientNet and delivers state-of-the-art performance with minimum time and space requirements. It is a single-scale detector similar to RetinaNet, which:

- uses EfficientNet as backbone;
- employs compound scaling;
- uses a newly proposed BiFPN, “efficient bidirectional cross-scale connections and weighted feature fusion”.

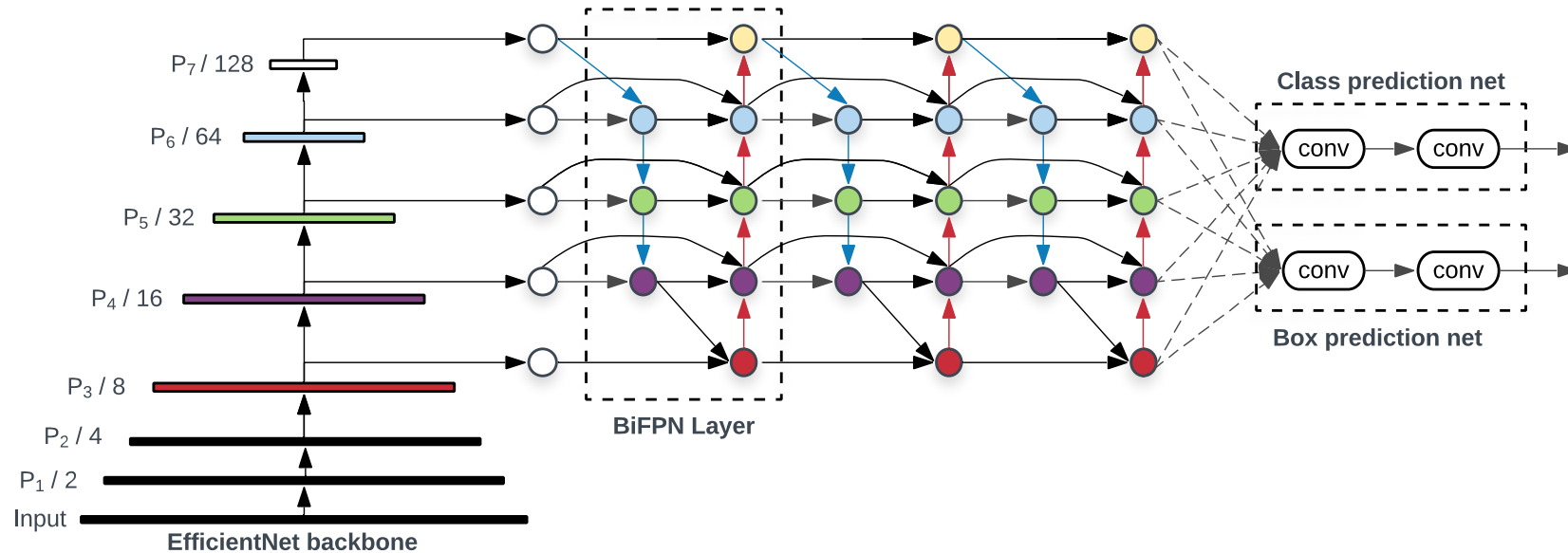


Figure 3 of paper "EfficientDet: Scalable and Efficient Object Detection", <https://arxiv.org/abs/1911.09070>.

In multi-scale fusion in FPN, information flows only from the pyramid levels with smaller resolution to the levels with higher resolution.

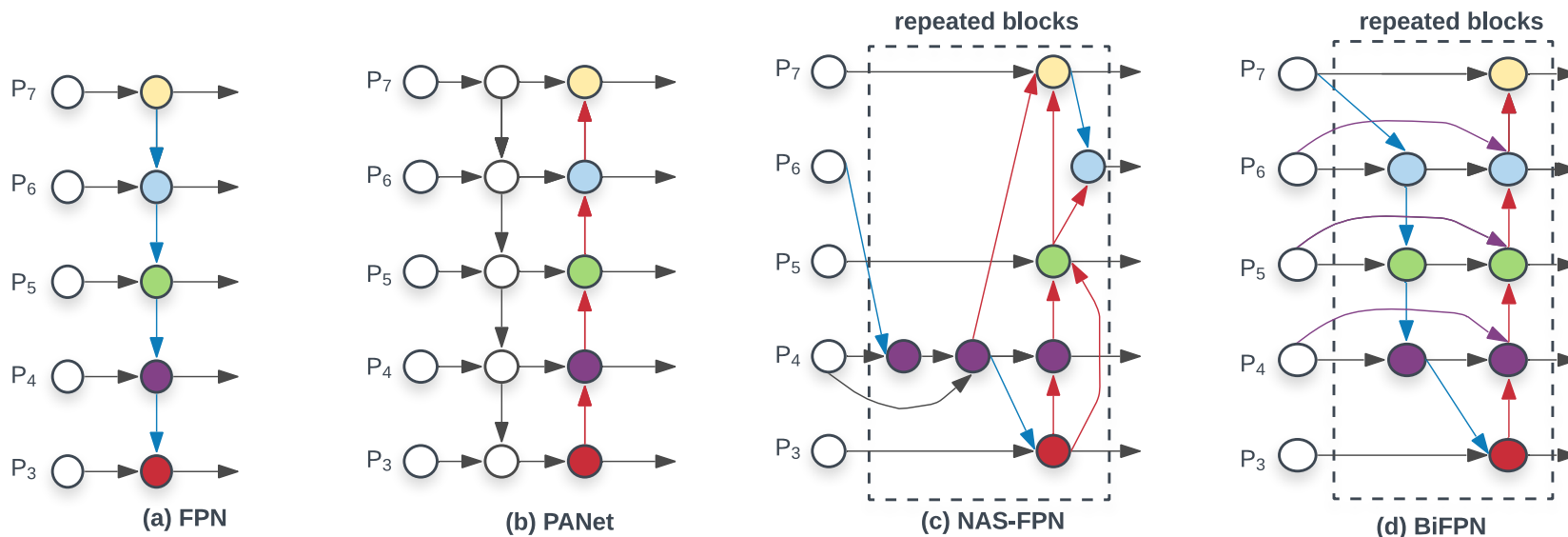


Figure 2 of paper "EfficientDet: Scalable and Efficient Object Detection", <https://arxiv.org/abs/1911.09070>.

BiFPN consists of several rounds of bidirectional flows. Each bidirectional flow employs residual connections and does not include nodes that have only one input edge with no feature fusion. All operations are 3×3 separable convolutions with batch normalization and ReLU, upsampling is done by repeating rows and columns and downsampling by max-pooling.

When combining features with different resolutions, it is common to resize them to the same resolution and sum them – therefore, both set of features is considered to be of the same importance. The authors however argue that features from different resolution contribute to the final result *unequally* and propose a combination with trainable weights.

- **Softmax-based fusion:** There is a trainable weight w_i for every input I_i and the final combination is

$$\sum_i \frac{e^{w_i}}{\sum_j e^{w_j}} I_i.$$

- **Fast normalized fusion:** Authors propose a simpler alternative of weighting:

$$\sum_i \frac{\text{ReLU}(w_i)}{\varepsilon + \sum_j \text{ReLU}(w_j)} I_i.$$

It uses $\varepsilon = 0.0001$ for stability and is up to 30% faster on a GPU.

EfficientDet – Compound Scaling

Similar to EfficientNet, authors propose to scale various dimensions of the network, using a single compound coefficient ϕ .

After performing a grid search:

- the width of BiFPN is scaled as $W_{BiFPN} = 64 \cdot 1.35^\phi$,
- the depth of BiFPN is scaled as $D_{BiFPN} = 3 + \phi$,
- the box/class predictor has the same width as BiFPN and depth $D_{class} = 3 + \lfloor \phi/3 \rfloor$,
- input image resolution increases according to $R_{image} = 512 + 128 \cdot \phi$.

	Input size R_{input}	Backbone Network	BiFPN		Box/class
			#channels W_{bifpn}	#layers D_{bifpn}	#layers D_{class}
D0 ($\phi = 0$)	512	B0	64	3	3
D1 ($\phi = 1$)	640	B1	88	4	3
D2 ($\phi = 2$)	768	B2	112	5	3
D3 ($\phi = 3$)	896	B3	160	6	4
D4 ($\phi = 4$)	1024	B4	224	7	4
D5 ($\phi = 5$)	1280	B5	288	7	4
D6 ($\phi = 6$)	1280	B6	384	8	5
D6 ($\phi = 7$)	1536	B6	384	8	5

Table 1 of paper "EfficientDet: Scalable and Efficient Object Detection", <https://arxiv.org/abs/1911.09070>.

EfficientDet – Results

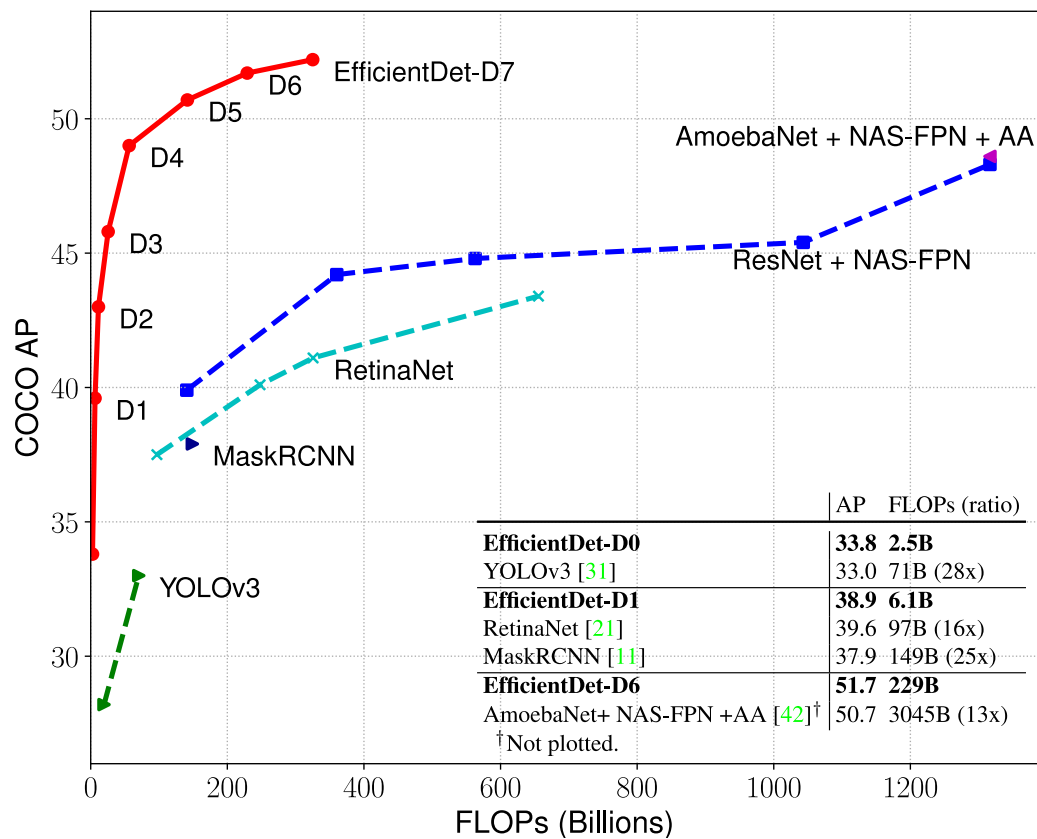


Figure 1 of paper "EfficientDet: Scalable and Efficient Object Detection", <https://arxiv.org/abs/1911.09070>.

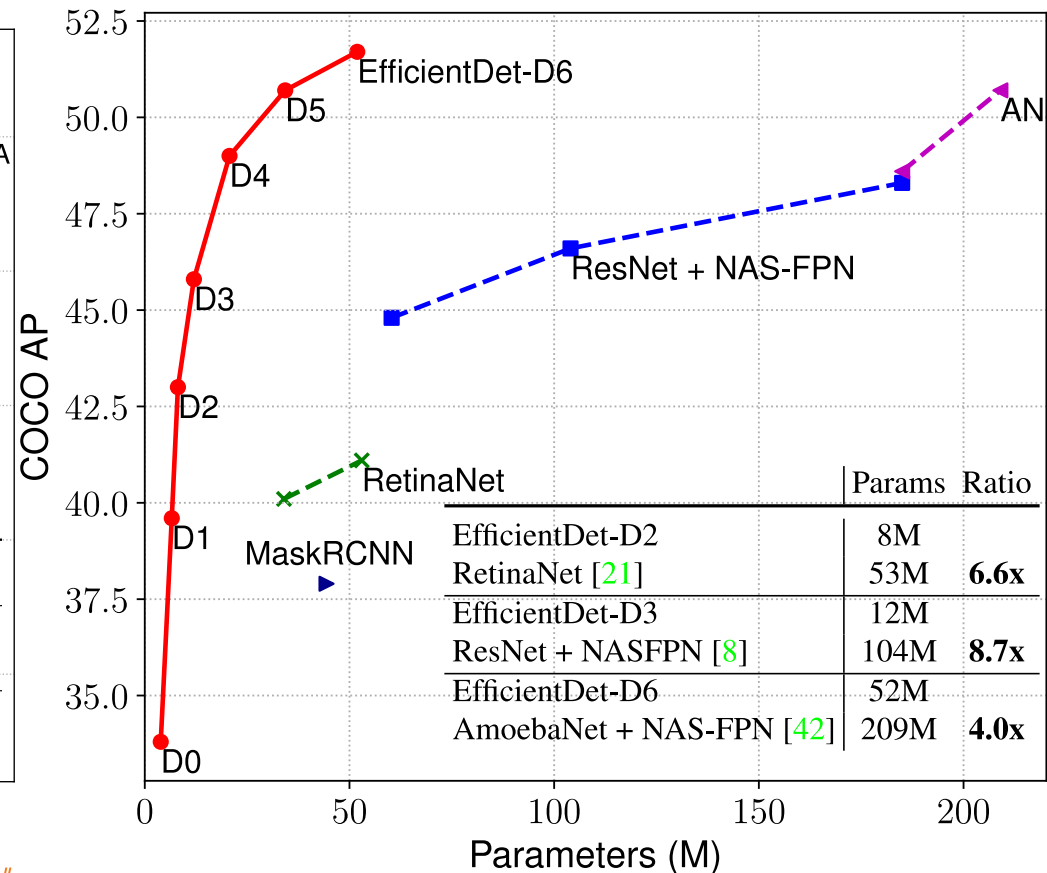


Figure 4 of paper "EfficientDet: Scalable and Efficient Object Detection", <https://arxiv.org/abs/1911.09070>.

Model	tet-dev			val	Params	Ratio	FLOPs	Ratio	Latency	
	AP	AP_{50}	AP_{75}	AP					GPU _{ms}	CPU _s
EfficientDet-D0 (512)	33.8	52.2	35.8	33.5	3.9M	1x	2.5B	1x	16	0.32
YOLOv3 [31]	33.0	57.9	34.4	-	-	-	71B	28x	51 [†]	-
EfficientDet-D1 (640)	39.6	58.6	42.3	39.1	6.6M	1x	6.1B	1x	20	0.74
RetinaNet-R50 (640) [21]	37.0	-	-	-	34M	6.7x	97B	16x	27	2.8
RetinaNet-R101 (640)[21]	37.9	-	-	-	53M	8.0x	127B	21x	34	3.6
EfficientDet-D2 (768)	43.0	62.3	46.2	42.5	8.1M	1x	11B	1x	24	1.2
RetinaNet-R50 (1024) [21]	40.1	-	-	-	34M	4.3x	248B	23x	51	7.5
RetinaNet-R101 (1024) [21]	41.1	-	-	-	53M	6.6x	326B	30x	65	9.7
ResNet-50 + NAS-FPN (640) [8]	39.9	-	-	-	60M	7.5x	141B	13x	41	4.1
EfficientDet-D3 (896)	45.8	65.0	49.3	45.9	12M	1x	25B	1x	42	2.5
ResNet-50 + NAS-FPN (1024) [8]	44.2	-	-	-	60M	5.1x	360B	15x	79	11
ResNet-50 + NAS-FPN (1280) [8]	44.8	-	-	-	60M	5.1x	563B	23x	119	17
ResNet-50 + NAS-FPN (1280@384)[8]	45.4	-	-	-	104M	8.7x	1043B	42x	173	27
EfficientDet-D4 (1024)	49.4	69.0	53.4	49.0	21M	1x	55B	1x	74	4.8
AmoebaNet+ NAS-FPN +AA(1280)[42]	-	-	-	48.6	185M	8.8x	1317B	24x	259	38
EfficientDet-D5 (1280)	50.7	70.2	54.7	50.5	34M	1x	135B	1x	141	11
EfficientDet-D6 (1280)	51.7	71.2	56.0	51.3	52M	1x	226B	1x	190	16
AmoebaNet+ NAS-FPN +AA(1536)[42]	-	-	-	50.7	209M	4.0x	3045B	13x	608	83
EfficientDet-D7 (1536)	52.2	71.4	56.3	51.8	52M	1x	325B	1x	262	24

We omit ensemble and test-time multi-scale results [27, 10].

[†]Latency marked with [†] are from papers, and others are measured on the same machine with Titan V GPU.

Table 2 of paper "EfficientDet: Scalable and Efficient Object Detection", <https://arxiv.org/abs/1911.09070>.

EfficientDet – Latencies

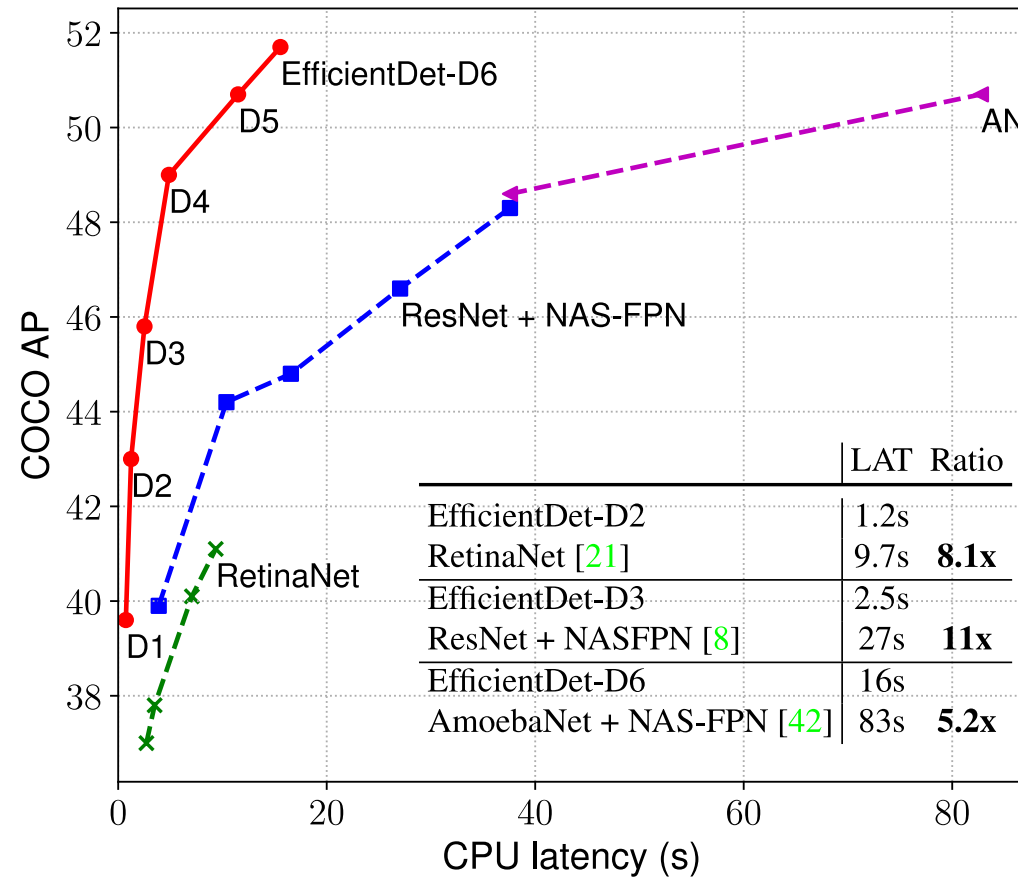
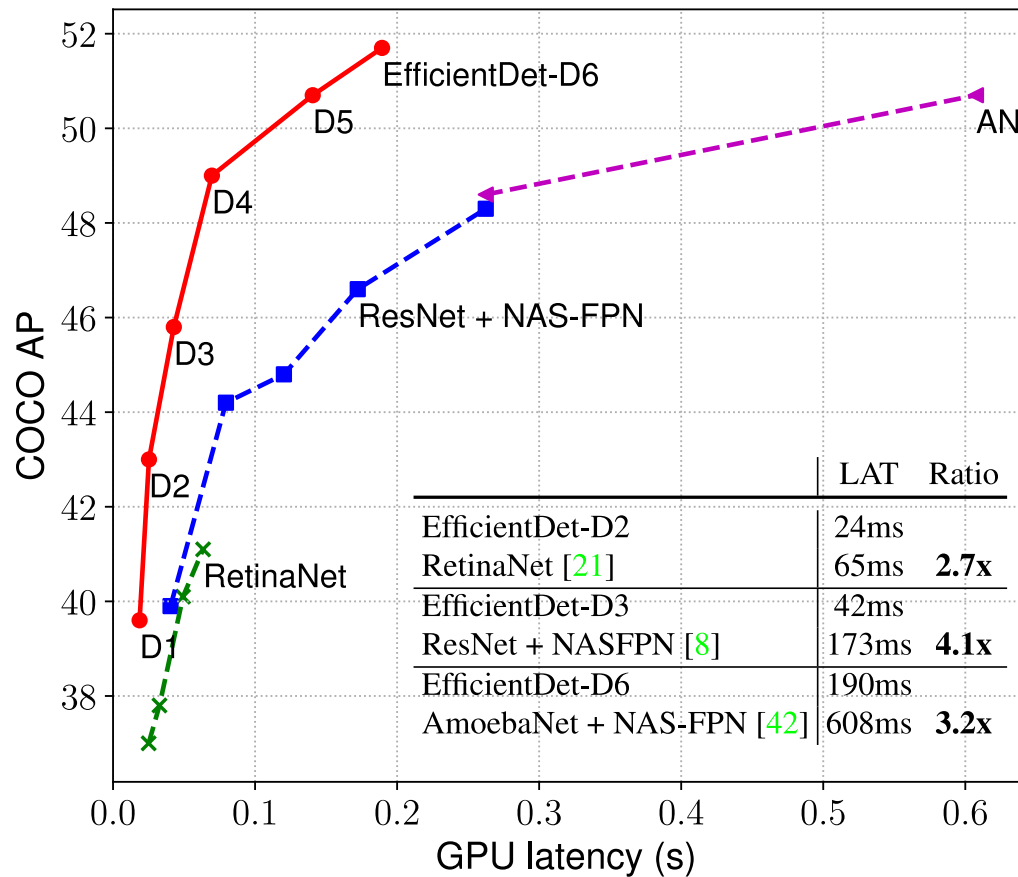


Figure 4 of paper "EfficientDet: Scalable and Efficient Object Detection", <https://arxiv.org/abs/1911.09070>.

Given that EfficientDet employs both a powerful backbone and new BiFPN, authors quantify the improvement of the individual components.

	AP	Parameters	FLOPs
ResNet50 + FPN	37.0	34M	97B
EfficientNet-B3 + FPN	40.3	21M	75B
EfficientNet-B3 + BiFPN	44.4	12M	24B

Table 4 of paper "EfficientDet: Scalable and Efficient Object Detection", <https://arxiv.org/abs/1911.09070>.

Furthermore, they provide comparison with previously used cross-scale fusion architectures.

	AP	#Params ratio	#FLOPs ratio
Repeated top-down FPN	42.29	1.0x	1.0x
Repeated FPN+PANet	44.08	1.0x	1.0x
NAS-FPN	43.16	0.71x	0.72x
Fully-Connected FPN	43.06	1.24x	1.21x
BiFPN (w/o weighted)	43.94	0.88x	0.67x
BiFPN (w/ weighted)	44.39	0.88x	0.68x

Table 5 of paper "EfficientDet: Scalable and Efficient Object Detection", <https://arxiv.org/abs/1911.09070>.

Batch Normalization

Neuron value is normalized across the minibatch, and in case of CNN also across all positions.

Layer Normalization

Neuron value is normalized across the layer.

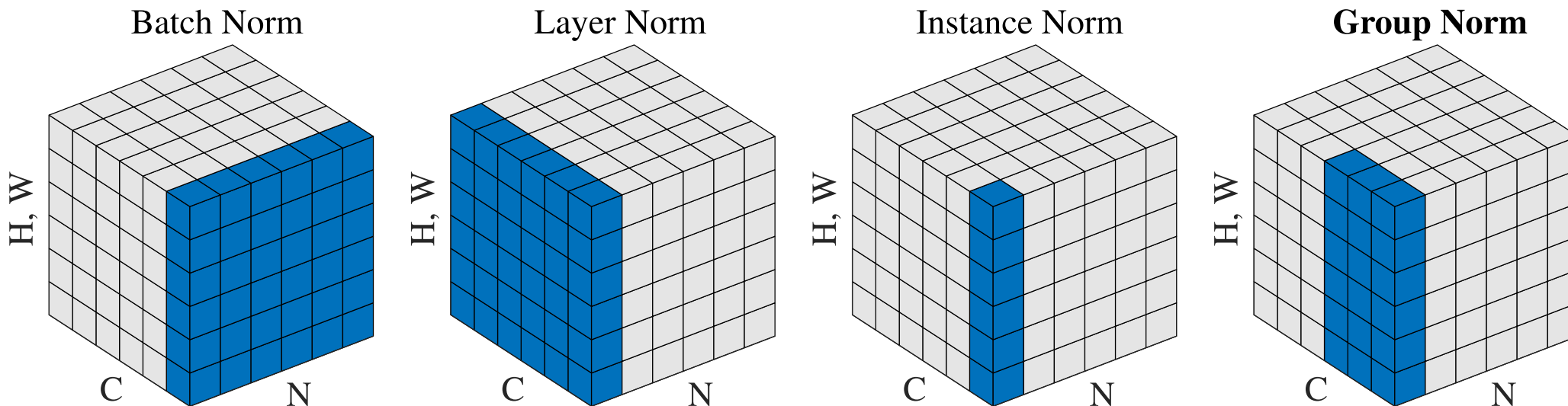


Figure 2 of paper "Group Normalization", <https://arxiv.org/abs/1803.08494>.

Group Normalization

Group Normalization is analogous to Layer normalization, but the channels are normalized in groups (by default, $G = 32$).

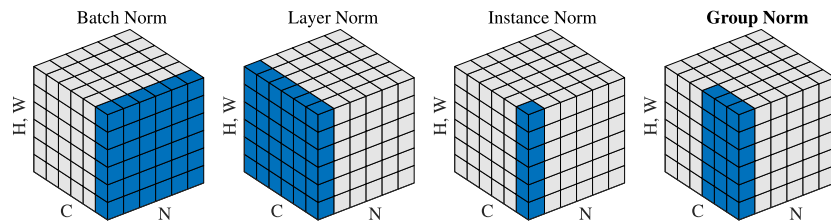


Figure 2 of paper "Group Normalization", <https://arxiv.org/abs/1803.08494>.

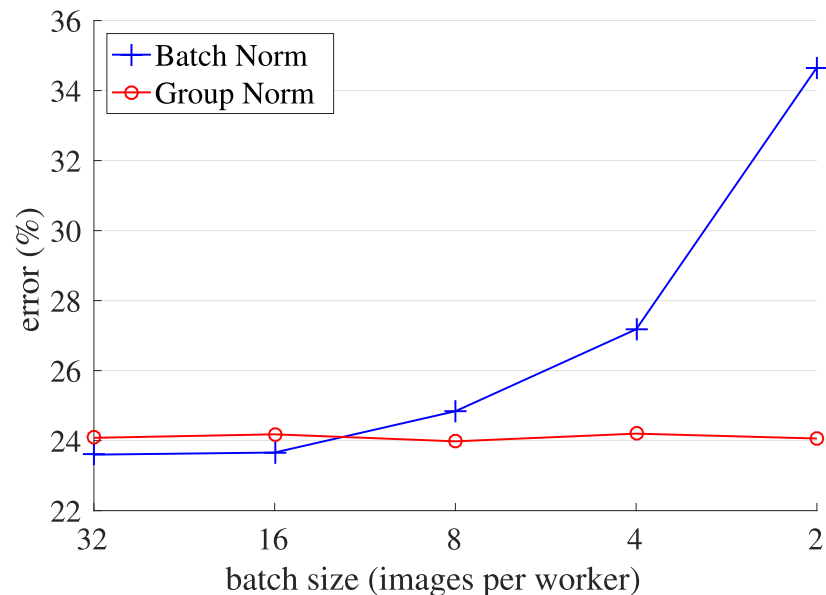


Figure 1 of paper "Group Normalization", <https://arxiv.org/abs/1803.08494>.

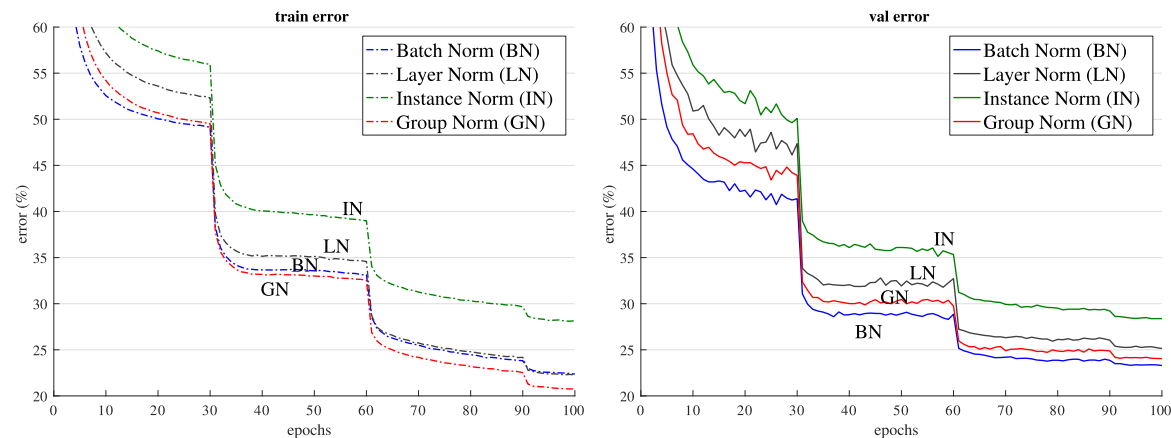


Figure 4. Comparison of error curves with a batch size of 32 images/GPU. We show the ImageNet training error (left) and validation error (right) vs. numbers of training epochs. The model is ResNet-50.

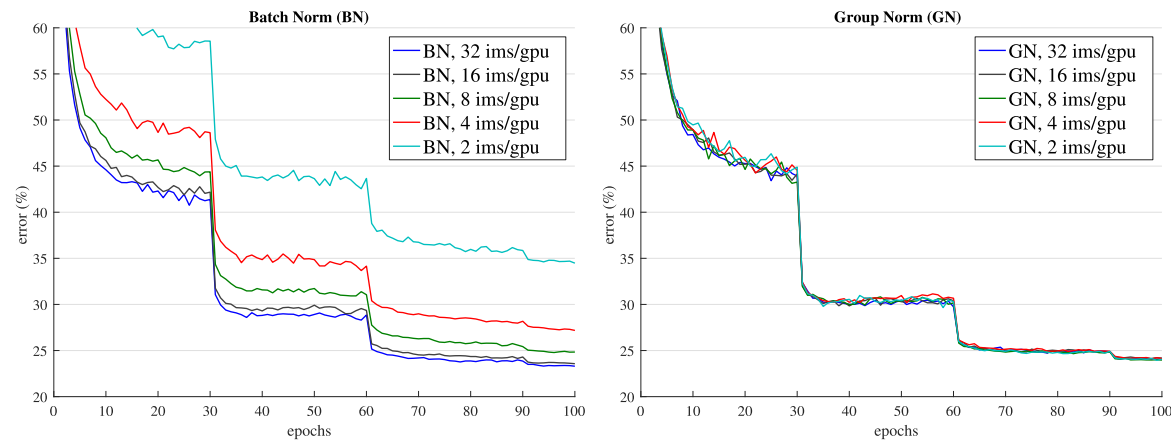


Figure 5. Sensitivity to batch sizes: ResNet-50's validation error of BN (left) and GN (right) trained with 32, 16, 8, 4, and 2 images/GPU.

Figures 4 and 5 of paper "Group Normalization", <https://arxiv.org/abs/1803.08494>.

backbone	AP^{bbox}	AP_{50}^{bbox}	AP_{75}^{bbox}	AP^{mask}	AP_{50}^{mask}	AP_{75}^{mask}
BN*	37.7	57.9	40.9	32.8	54.3	34.7
GN	38.8	59.2	42.2	33.6	55.9	35.4

Table 4. **Detection and segmentation results in COCO**, using Mask R-CNN with **ResNet-50 C4**. BN* means BN is frozen.

backbone	box head	AP^{bbox}	AP_{50}^{bbox}	AP_{75}^{bbox}	AP^{mask}	AP_{50}^{mask}	AP_{75}^{mask}
BN*	-	38.6	59.5	41.9	34.2	56.2	36.1
BN*	GN	39.5	60.0	43.2	34.4	56.4	36.3
GN	GN	40.0	61.0	43.3	34.8	57.3	36.3

Table 5. **Detection and segmentation results in COCO**, using Mask R-CNN with **ResNet-50 FPN** and a 4conv1fc bounding box head. BN* means BN is frozen.

Tables 4 and 5 of paper "Group Normalization", <https://arxiv.org/abs/1803.08494>.